X-ray nanodiffraction at individual SiGe/Si(001) dot molecules and its numerical description based on kinematical scattering theory

M. Dubslaff,[1] M. Hanke,[1,a)] S. Schöder,[2] M. Burghammer,[2] T. Boeck,[3] and J. Patommel[4]
[1]*Paul-Drude-Institut für Festkörperelektronik, Hausvogteiplatz 5-7, D-10117 Berlin, Germany*
[2]*European Synchrotron Radiation Facility, BP 220, F-38043 Grenoble Cedex, France*
[3]*Leibniz-Institut für Kristallzüchtung, Max-Born-Straße 2, D-12489 Berlin, Germany*
[4]*Institut für Strukturphysik, Technische Universität Dresden, Zellescher Weg 16, D-01069 Dresden, Germany*

(Received 17 February 2010; accepted 4 March 2010; published online 30 March 2010)

Individual self-assembled SiGe/Si(001) dot molecules were investigated by scanning x-ray nanodiffraction with a beam size of 250 nm in diameter (full width at half maximum). The samples contain dot molecules with either one, two, three, or four dots. Different azimuthal configurations were measured and compared with simulated diffraction patterns. We have combined finite element calculations, kinematic scattering simulations, and experimental measurements to obtain information about lateral positional correlation as well as strain and germanium content within individual dot molecules. © *2010 American Institute of Physics*. [doi:10.1063/1.3373916]

X-ray diffraction with micrometer or even millimeter-sized beams inherently suffers from a statistical average over many objects—a drawback, which can be overcome with smaller spot sizes. In recent years highly brilliant micro- and nanofocused x-ray beams became feasible at synchrotron radiation sources by the use of, e.g., Kirkpatrick–Baez (KB) mirrors,[1] Fresnel zone plates,[2] or refractive x-ray lenses.[3–5] This development promotes analytical techniques like scanning transmission x-ray microscopy[6] and microtomography.[7] Further on, one may combine the excellent resolution in real space (given by the x-ray spot) with a high resolution in angular space (e.g., by using a two-dimensional detector). The spot size defines the excited region at the sample, whereas the high angular resolution provides detailed information about the lattice parameters and positional correlations within the structures at the illuminated area. Thus, scanning x-ray nanodiffraction enables the investigation of *individual* nanoscaled objects like quantum dots[8–10] or quantum wires[11] and provides spatially resolved strain distribution and chemical composition.

In this study we have focused on SiGe/Si(001) dot molecules (DM), which self-assemble around small cavities, Fig. 1. The individual SiGe dots are grown self-organized in the so-called Stranski–Krastanow growth mode by means of liquid phase epitaxy. In a first step a Si-rich (98.5%) SiGe layer was established on a Si(001) substrate. This yields small pyramidlike cavities, which subsequently serve as a template for the formation of DMs. For further details of the growth process see Ref. 12. The interplay between elastic strain caused by the heteroepitaxial misfit, its relaxation and the particular shape of the cavities leads to DMs consisting of either one (not shown), two [denoted F1 and F2 in Fig. 1(a)], three (b) or four SiGe dots (c). It is interesting to note that the dot nucleation performs at the cavity edges due to efficient relaxation (minima of the elastic strain energy) in ⟨110⟩ direction. With their size (comparable to the size of the x-ray spot) and their inherent strain symmetry this type of DMs is particularly suited for our kind of methodical study.

Figure 2 depicts the two Cartesian elastic displacements $\Delta x/a_{Si}$ (lateral) and $\Delta z/a_{Si}$ (vertical) as numerically calculated by finite element method (FEM). The lateral displacement (bottom) shows that strain relaxation happens more effectively toward the cavity (toward the center of the molecule) than in the opposite direction, hence along the planar substrate. This can clearly be seen in the bottom of Fig. 2(b) by comparing the extension of features D1 and D2. For symmetry reasons this holds as well for the orthogonal in-plane direction $[\bar{1}10]$ (not shown).

Diffraction experiments have been performed at beamline ID13 of the European Synchrotron Radiation Facility (ESRF) in Grenoble, France. We have used monochromatic x-rays with an energy E of 12.4 keV ($\Delta E/E=10^{-4}$), which were highly focused by KB mirrors into a 250 nm spot (full width at half maximum). A two-dimensional Fast Readout Low Noise detector with a pixel size of 50 μm was placed 920 mm behind the sample, Fig. 3. The recorded diffraction patterns represent two-dimensional sections through reciprocal space. For a given setup only one in-plane direction of the elastic strain distribution can be probed, namely the direction, which is contained within the diffraction plane.

We have measured diffusely scattered intensities around the Si(004) reflection at various locations at the sample covering all different types of DMs. In Fig. 4 a typical sample translation scan, as illustrated in Fig. 3, with a step width of 200 nm and an exposure time of 10 s is shown. The sample

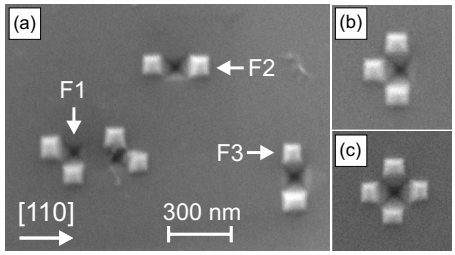

FIG. 1. Scanning electron micrographs of SiGe/Si(001) Dot molecules self-assembled on cavities, namely the two types of bimolecules (a) denoted F1 and F2, a trimolecule (b) and highly symmetric quadruplets (c).

a)Electronic mail: hanke@pdi-berlin.de.

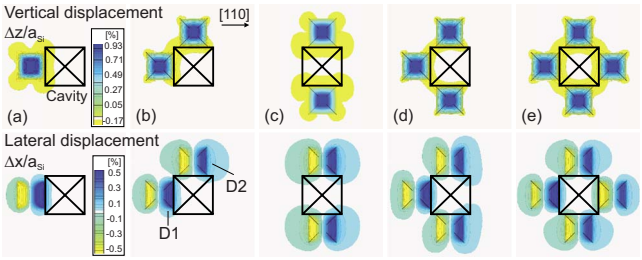

FIG. 2. (Color online) Elastic strain relaxation due to heteroepitaxial lattice mismatch within and around different DMs (a)–(e) calculated by FEM. Pictures in the first row show the relative displacement along the surface normal [001]; on the second row the lateral component $\Delta x/a_{\mathrm{Si}}$ in [110] direction is depicted. In the center of each image the pyramidlike cavity is sketched.

was scanned along $[\bar{1}10]$, which refers to a spatial resolution (in this direction) comparable to the beam size of 250 nm. Due to the beam's footprint on the sample the resolution perpendicular deteriorates to around 680 nm. In this example of an illuminated quadruplet a honeycomblike diffraction pattern appears and disappears within three steps. While scanning the sample across several micrometer the beam mostly illuminates just the Si(001) substrate without DMs and does not cause such complex diffraction patterns (e.g., first and last frame in Fig. 4). If the spot illuminates the DM a rather weak SiGe reflection appears at lower q_z (not shown here). The DM density calculated from the electron micrographs, 0.8 $\mu\mathrm{m}^{-2}$, and from the observed diffraction patterns during a translation scan, 0.9 $\mu\mathrm{m}^{-2}$, are in good agreement.

In order to extract the particular type of DM as well as to probe its structural parameters (chemical composition versus elastic strain) we have performed kinematical scattering simulations.[13] The three-dimensional displacement field obtained from the FEM calculations in Fig. 2 is used as an input. In kinematical theory one can obtain the scattering at a particular point in reciprocal space just by adding up coherently the scattering by all illuminated scatterers. Figure 5 compares now calculated diffraction patterns (middle) with experimental results (bottom) at bi- and tri-molecules of different azimuthal orientation (top). The honeycomb features and streaks generally originate from the lateral positional correlation among the individual SiGe dots. These correlation streaks are observable not only around the SiGe(004) reflection but as well around the intense Si(004) reflection since the strain relaxation fields of the SiGe dots affect the Si substrate directly below the DMs. A molecule consisting of two dots only causes extended streaks (S). Their inclination may serve as a fingerprint of the aziumthal DM orientation. This even holds for tri-molecules where the diffraction pattern is not invariant against different azimuths too, Figs. 5(c) and 5(d). Actually similar superstructure satellites are known

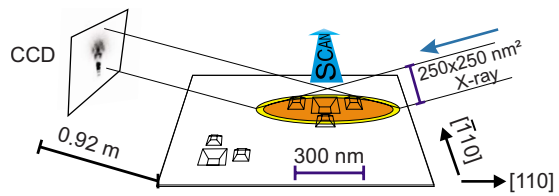

FIG. 3. (Color online) Sketch of the experimental setup. Scanning the sample along $[\bar{1}10]$ preserves a high spatial resolution while in the orthogonal [110] direction the beam's footprint impairs resolution.

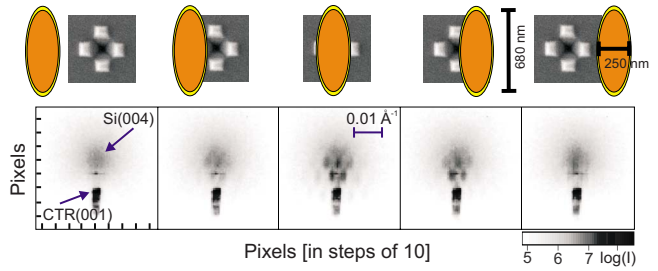

FIG. 4. (Color online) Diffraction patterns near the Si(004) substrate reflection. The sequence refers to a sample translation in real space along $[\bar{1}10]$ crossing a quadruplet. Note that the intensity distributions are plotted on a pixel scale. The scale bar gives a projection to the (001) plane and is, strictly speaking, only exact in the frame's center. Each frame contains the intersection with the crystal truncation rod (CTR) of the (001) surface. Above the CTR (at higher q_z) one can observe diffusely scattered intensity around the Si(004) reflection, which clearly depends on the illuminated area of the dot molecule.

from ensemble averages[14,15] using partially coherent x-rays. However, applying spot sizes comparable to structural dimensions enables a highly local probe.

In the simulations Figs. 5(a) and 5(b), performed on the bi-molecules with directly adjacent dots, one can easily study the influence of rotating the DM by 90°: the correlation streaks (S) change their direction as well. From a first view the reader might expect a 45° inclination considering a perfect DM of two identical dots aligned in ⟨100⟩ direction. However, the intensity patterns shown here do not contain the (001) surface normal since the detector array probes an inclined (and slightly curved) section of the reciprocal space. Thus, for our setup the streaks appear under an angle of 68.5°. A further simulation (not shown) of the q_x-q_y in-plane section reveals streaks inclined by 45°.

The separation Δq of the maxima corresponds to the distance Δx between the dots in the DM in real space via: $\Delta x = 2\pi/\Delta q$. In the simulated reciprocal space map for an incident beam (more accurate its projection on the sample surface) along [110] illuminating two neighboring dots, see middle of Figs. 5(a) and 5(b), the satellites are separated by $\Delta q = 0.0042$ Å^{-1}, which corresponds to an inter-dot distance of about 150 nm in real space.

The DM formation of Figs. 5(c) and 5(d) can be considered as a combination of the two DMs depicted in Figs. 5(a) and 5(b) with two neighboring dots each. This becomes also

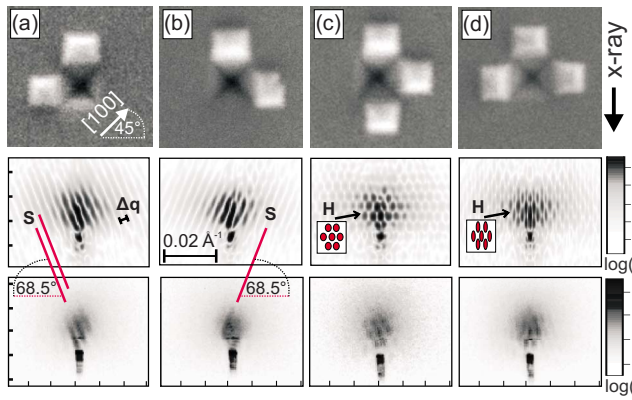

FIG. 5. (Color online) Various configurations with two or three dots (top), corresponding scattering simulations based on FEM models (center) and equivalent regions in reciprocal space (bottom). As in Fig. 4, the measured (and calculated) intensities are plotted on a pixel scale (20 pixels per tick).

prominent in the simulated diffraction pattern, where the diffusely scattered intensity from the DM in Figs. 5(c) and 5(d) may be interpreted as a superposition of the diffraction images in Figs. 5(a) and 5(b). The (vertically elongated) spot in (d) can be ascribed to the shorter extension of the DM in this direction in real space.

Configurations with opposite dots, Fig. 1(a) and those with four dots have been simulated as well (not shown). In these calculations the formation F2 yields vertical streaks whereas formation F3 induces horizontal ones. Finally the diffraction pattern of a quadruplet, Fig. 1(c), shows a honeycomblike structure comparable to the formations with three pyramids.

By varying the FEM model and comparing the resulting scattering simulation with the measured data, the germanium content in the SiGe dots can be examined. In our simulations the model, which corresponds to 26% Ge, 74% Si, appears to be in best agreement with the experimental data, $q_{001}^{\mathrm{SiGe}} = 4.58\ \text{Å}^{-1}$.

In summary, we have reported spatially resolved x-ray diffraction on various SiGe/Si(001) DMs by means of nanofocused x-ray beams. The proposed method enables a destruction-free local probe of elastic strain (and hence chemical composition) at a 250 nm scale. Since the scattering process is fully coherent within the x-ray spot, it is possible to relate the diffraction patterns to a particular configuration. From numerical scattering simulations we have obtained a germanium content of 26% within the individual dots. This values appears to be independent of the number of dots contained in a DM. Further on the orientation of bi- and trimolecules toward the beam could be determined.

We acknowledge the German Research Foundation (DFG) for financial support, Project No. HA3495/6-1, the European Synchrotron Radiation Facility for financial and technical support during experiment SI-1784 and F. Heyroth, Martin-Luther-Universität Halle-Wittenberg for providing the SEM images of the samples.

[1] K. Yamamura, K. Yamauchi, H. Mimura, Y. Sano, A. Saito, K. Endo, A. Souvorov, M. Yabashi, K. Tamasaku, T. Ishikawa, and Y. Mori, Rev. Sci. Instrum. **74**, 4549 (2003).
[2] C. David, B. Nöhammer, and E. Ziegler, Microelectron. Eng. **61-62**, 987 (2002).
[3] A. Snigirev, V. Kohn, I. Snigireva, and B. Lengeler, Nature (London) **384**, 49 (1996).
[4] B. Lengeler, C. G. Schroer, J. Tümmler, B. Benner, M. Richwin, A. Snigirev, I. Snigireva, and M. Drakopoulos, J. Synchrotron Radiat. **6**, 1153 (1999).
[5] C. G. Schroer, O. Kurapova, J. Patommel, P. Boye, J. Feldkamp, B. Lengeler, M. Burghammer, C. Riekel, L. Vincze, A. van der Hart, and M. Küchler, Appl. Phys. Lett. **87**, 124103 (2005).
[6] F. Pfeiffer, C. David, J. F. van der Veen, and C. Bergmann, Phys. Rev. B **73**, 245331 (2006).
[7] C. G. Schroer, J. Meyer, M. Kuhlmann, B. Benner, T. F. Günzler, B. Lengeler, C. Rau, T. Weitkamp, A. Snigirev, and I. Snigireva, Appl. Phys. Lett. **81**, 1527 (2002).
[8] M. Hanke, M. Dubslaff, M. Schmidbauer, T. Boeck, S. Schöder, M. Burghammer, C. Riekel, J. Patommel, and C. G. Schroer, Appl. Phys. Lett. **92**, 193109 (2008).
[9] C. Mocuta, J. Stangl, K. Mundboth, T. H. Metzger, G. Bauer, I. A. Vartanyants, M. Schmidbauer, and T. Boeck, Phys. Rev. B **77**, 245425 (2008).
[10] T. Scheler, M. Rodrigues, T. W. Cornelius, C. Mocuta, A. Malachias, R. Magalhaes-Paniago, F. Comin, J. Chevrier, and T. H. Metzger, Appl. Phys. Lett. **94**, 023109 (2009).
[11] A. Davydok, A. Biermanns, U. Pietsch, J. Grenzer, H. Paetzelt, V. Gottschalch, and J. Bauer, J. Synchrotron Radiat. **16**, 1704 (2009).
[12] M. Hanke, T. Boeck, A.-K. Gerlitzke, F. Syrowatka, and F. Heyroth, Appl. Phys. Lett. **88**, 063119 (2006).
[13] T. Wiebach, M. Schmidbauer, M. Hanke, H. Raidt, R. Köhler, and H. Wawra, Phys. Rev. B **61**, 5571 (2000).
[14] M. Hanke, M. Schmidbauer, and R. Köhler, J. Appl. Phys. **96**, 1959 (2004).
[15] I. A. Vartanyants, I. K. Robinson, J. D. Onken, M. A. Pfeifer, G. J. Williams, F. Pfeiffer, T. H. Metzger, and Z. Zhong, Phys. Rev. B **71**, 245302 (2005).